TU Delft

Delft University of Technology

Document Version
Final published version

Licence
Dutch Copyright Act (Article 25fa)

Citation (APA)
Korswagen, P. A., Longo, M., & Rots, J. G. (2026). Modelling of Light Damage to Façades from Combined Soil Curvature and Horizontal Strain. In S. Saloustros, & K. Beyer (Eds.), *Structural Analysis of Historical Constructions: SAHC 2025, Volume 1* (pp. 946–960). (RILEM Bookseries; Vol. 64). Springer. https://doi.org/10.1007/978-3-032-13469-1_75

Important note
To cite this publication, please use the final published version (if applicable).
Please check the document version above.

Copyright
In case the licence states “Dutch Copyright Act (Article 25fa)”, this publication was made available Green Open Access via the TU Delft Institutional Repository pursuant to Dutch Copyright Act (Article 25fa, the Taverne amendment). This provision does not affect copyright ownership.
Unless copyright is transferred by contract or statute, it remains with the copyright holder.

Sharing and reuse
Other than for strictly personal use, it is not permitted to download, forward or distribute the text or part of it, without the consent of the author(s) and/or copyright holder(s), unless the work is under an open content license such as Creative Commons.

Takedown policy
Please contact us and provide details if you believe this document breaches copyrights.
We will remove access to the work immediately and investigate your claim.

This work is downloaded from Delft University of Technology.

Modelling of Light Damage to Façades from Combined Soil Curvature and Horizontal Strain

Paul A. Korswagen(✉), Michele Longo, and Jan G. Rots

Faculty of Civil Engineering and Geosciences, Delft University of Technology, Delft, The Netherlands
p.a.korswagen@tudelft.nl

Abstract. Historical buildings in the Netherlands are often founded on shallow, unreinforced foundations atop soft soils such as peat, clay, or loam, making them vulnerable to ground movements. These movements can result from autonomous settlements due to the building's own weight, or from changes in the soil related to water table variations. Such sources typically induce differential vertical displacements, expressed as ground surface curvature. Movements from deeper sources, such as mining or tunnelling, also cause horizontal displacements or surface strains.

Masonry buildings are sensitive to strains from restrained shrinkage, temperature fluctuations, and soil movements. This study examines façade damage due to a combination of curvature and horizontal strain imposed through the foundations. Non-linear models of masonry façades were placed on a deformable soil block, whose boundaries were manipulated to create targeted combinations of curvature and strain at the surface.

The analysis of various combinations showed that while curvature and horizontal strain each cause damage—manifested as cracks in the masonry—their combination amplifies it. For instance, cracks 1 mm wide appear at a tensile strain of 5e−4 (0.5 mm/m), but when combined with an angular distortion of 1e−3 rad, only half that strain is needed to produce similar damage.

Understanding how curvature and strain interact to damage façades helps define safer deformation limits for vulnerable historical buildings, particularly in areas affected by water table regulation or mining. Additionally, the initial condition of structures must be considered when evaluating their vulnerability to external hazards, including seismic activity.

Keywords: Historical Masonry · Ground Displacements · Crack-based Damage · FEM

1 Introduction

Historical façades are exposed to a multitude of hazards, ranging from ground settlements to earthquake vibrations [1–4]. These can cause damage which also accumulates over time [5, 6]. In masonry façades, typical throughout the Netherlands, this type of damage

© The Author(s), under exclusive license to Springer Nature Switzerland AG 2026
S. Saloustros and K. Beyer (Eds.): SAHC 2025, RILEM Bookseries 64, pp. 946–960, 2026.
https://doi.org/10.1007/978-3-032-13469-1_75

becomes visible as cracks [7]. Small cracks are sealed to restore the watertightness of the façade and prevent additional damage [8]. The initial condition of a structure is key to analyse its subsequent response. When evaluating the effect of seismicity, for example, pre-damaged façades will become more flexible. In the Netherlands, the behaviour of masonry façades during the crack initiation and early propagation stages is of interest [9]. Here, light earthquake vibrations, in the order of 2 to 20 mm/s (as Peak Ground Velocity), are known to cause damage to all types of unreinforced masonry structures [10]. To accurately predict the degree of damage, and more importantly, of damage aggravation, it is necessary to account for the initial condition of the structure [11].

When considering the (initial) causes of damage, settlements are an important source [12–19]. Typically, nearby trees, construction, or renovation activities are mostly responsible [20, 21]. Additionally, changes in the water table may lead to varying soil behaviour which, in combination with the weight of the buildings, will lead to differential settlements [22]. For planar façades, these deformations are well represented by the curvature of the ground surface leading to angular distortions of the façade [23]. Several studies and guidelines exist to estimate safe limits of distortions for building façades [24–26]; however, historical masonry façades, built of unreinforced masonry for both wall and foundation are especially vulnerable.

Furthermore, ground deformations are not limited to local curvatures of the soil at the scale of the buildings; when deep mining activities are ongoing, such as gas or salt mining, subsidence on a kilometre-scale is expected. These vertical deformations lead to negligible curvatures at the building scale but are associated with important horizontal strains instead [27, 28]. If tensile horizontal strains are transferred to the façades, see Fig. 1, their large stiffness and limited tensile strength, is likely to result in damage.

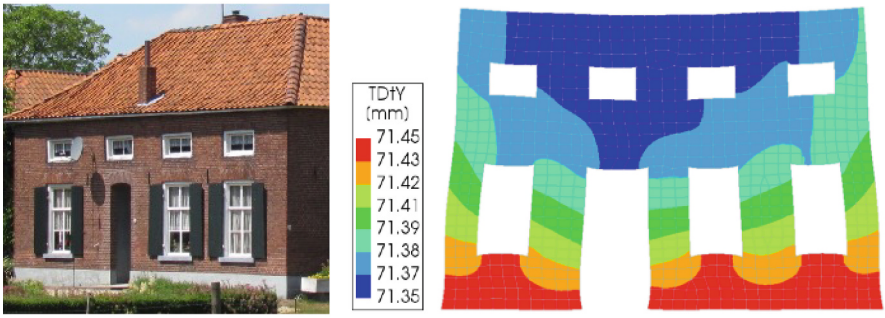


Fig. 1. An example of a historical masonry façade, left. Right, a planar model with an extension horizontal strain applied to the foundation.

Estimating damage from applied horizontal strains is straightforward if a conservative approach is sufficient where the strains are fully transferred to the façade. Some studies suggest that about 30% may be transferred to buildings [29]. Yet, this will depend on the relationship between the stiffness of the façade and of the neighbouring soil. Figure 2 shows how the interaction between the structure and the soil also plays a role. If the soil is much stiffer than the building, then the structure will be forced to deform

with the soil, leading to damage. Modification factors [30] that relate the greenfield displacements (the ground deformation without the building) to the displacement with the building, are often used to estimate the soil-structure interaction.

Nevertheless, modification factors do not account for the varying stiffness of a building. As a façade becomes damaged, it also becomes more flexible, allowing a higher transfer of the horizontal soil strain. Furthermore, data on expected damage due to a combination of soil curvature and horizontal strain is scarce. Boscardin and Cording [31] formulate thresholds for greenfield curvature and strain based on empirically collected data. This approach, however, is not specific to historical masonry Dutch façades, it cannot provide probabilities of damage initiation, and is constrained by the limited damage supporting the proposed thresholds.

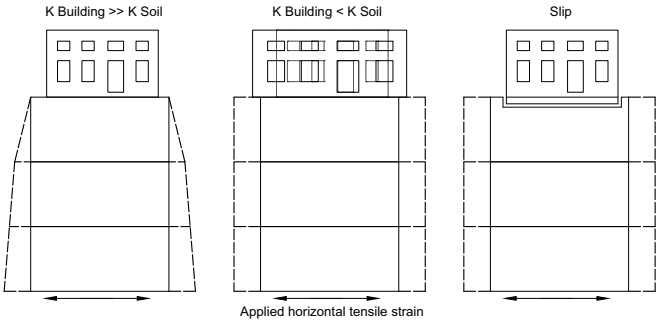


Fig. 2. Left, situation when the building is much stiffer than the soil; middle, the soil is stiffer than the structure; and right, when slip at the interface between structure and soil occurs. K refers to the stiffness of the material.

In this paper, we present the outcome of an extensive study that aimed to consider several complexities for estimation damage on unreinforced masonry buildings on unreinforced, shallow foundations. First, any combination of soil curvature and horizontal is considered. Second, the soil-structure interaction, which limits the transfer of deformation to the building, is realistically portrayed. Third, progressive damage of the façade is depicted and in turn affects the deformations of soil and building. Fourth, including sufficient variations of the façade and its properties, a probability for damage initiation at soil curvature/strain combinations can be provided.

2 Methods

Finite Element Method (FEM) numerical models are used to depict a masonry façade with its foundation embedded in a block of soil (Fig. 3). The façade includes its transversal walls, masonry lintel over the wide opening of the door, and shallow masonry foundation simplified to a rectangular cross section. The loads of the roof are applied to the transversal wall as depicted. The foundation is embedded into a soil block for which three alternatives are presented: a sandy soil over the height of the soil block (#6), a clay-based profile that includes shallow layers of sand and loam (#9), and an in-between profile with both clay and sand (#0).

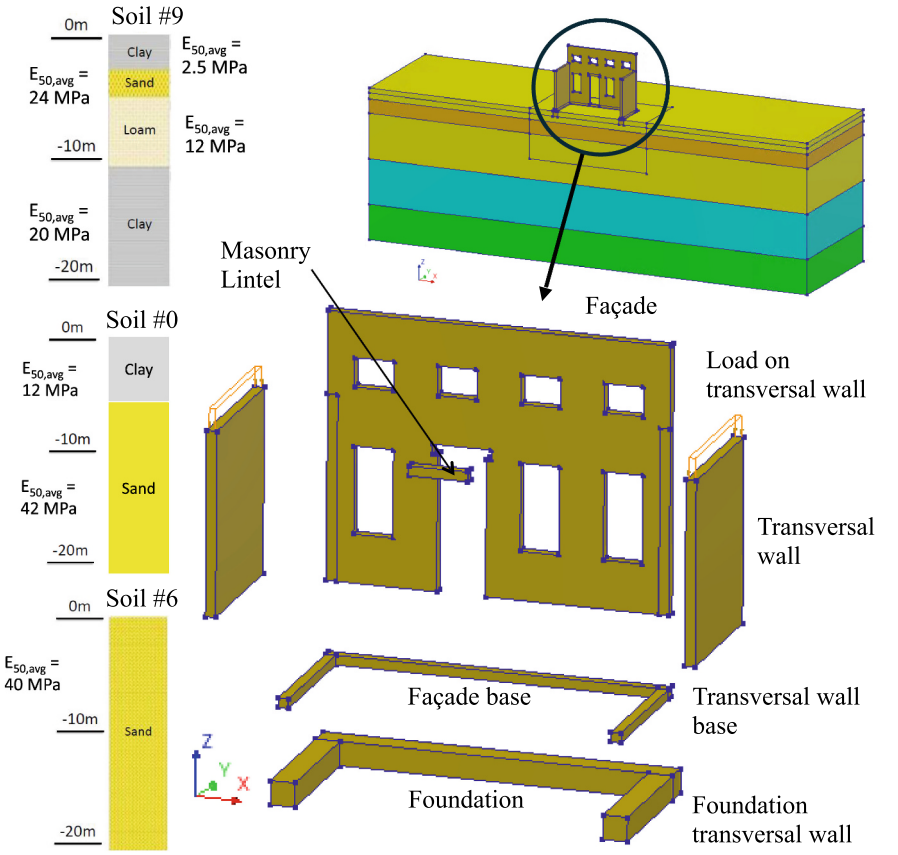


Fig. 3. Overview of the FEM model including the façade with its transversal walls, foundation, and soil block with multiple layers. The shallow foundation is embedded in the soil block, and the model is symmetric on the LxH plane. L = 45 m, H = 15 m, W = 12.5 m.

The soil block is also modelled using a non-linear material. Specifically, the Hardening Soil Model (Small-Strains), which presents a higher stiffness for small strains, is used [32]. This model requires multiple parameters, which are varied in depth and are presented in Table 1. The initial stiffness of the soil is higher (E0) which provides more transfer for small strains.

To reproduce the soil deformation, a two-tiered approach is ingeniously employed as depicted in Fig. 4. In a first step, the soil block, without the façade, is subjected to boundary displacements such that the deformations at the centre of the ground surface represent target greenfield values. The boundary displacements comprise varying vertical displacements at the bottom to reproduce a curvature at the surface and horizontal displacements at the lateral edges to fabricate horizontal strains. The applied displacements are such that 22 curvature/strain combinations are generated; see Fig. 5. For each soil profile, these combinations yield slightly different greenfield displacements due to the differing soil properties. The combinations include extension horizontal strains

Table 1. Derived values for input corresponding to the clay soil profile (#9) for the small-strains hardening soil model. Values in MPa where required. For variable names, see [32].

#	Depth [m]		Type	E50	Eoed	Eur	E0	pref	POP	c	φ[°]	ψ	K0	γ0.7
1	0.00	−3.00	Clay	2	2	10	72	0.1	0.01	0.005	23	0	0.62	1E−04
2	−3.00	−5.30	Sand	24	24	96	216			0	35	5	0.43	
3	−5.30	−11.30	Loam	12	12	48	108			0	30	0	0.50	
4	−11.30	−28.50	Clay	19	19	77	288			0.001	28	0	0.54	
5	−28.50	−30.70	Sand	180	180	720	1620			0	40	10	0.36	

(positive) linked to convex (hogging) curvatures and contraction horizontal strains (negative) associated with concave (sagging) curvatures. The sagging and hogging profiles also differ in shape being symmetric or asymmetric [33]. A pure extensive and contractive horizontal strain is also applied but, due to the layered soil properties, this results in small greenfield curvatures. Generating large pure horizontal strains (1e−3) is not possible since the soil would incur in non-linear behaviour.

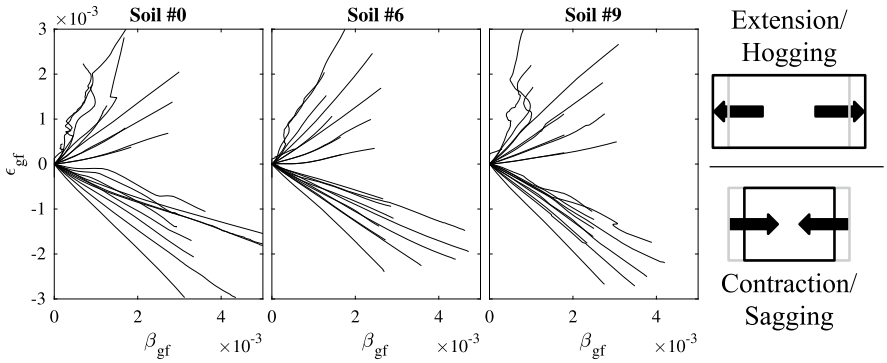


Fig. 5. Combinations of soil greenfield angular distortion (β) and horizontal strains (ε).

The second step involves applying identical boundary displacements to a soil block with a façade on top. In this manner, a relationship between the greenfield values (on the first-tier model) and the building response (second-tier model) is established. The dimensions of the soil block were chosen so that the presence of the buildings has only a negligible influence on the perimeter of the model; this is visible during the gravity loading stage, before boundary displacements are applied.

On the façade model, the soil displacements at the top (induced) will differ from the greenfield displacements; this is the influence of the building. If the façade is very flexible (because it has many openings or several cracks), these displacements will be similar. On the building, the measured strain and distortion can be reported. More importantly, the cracking behaviour of the masonry façade are characterised using Ψ, a crack-based

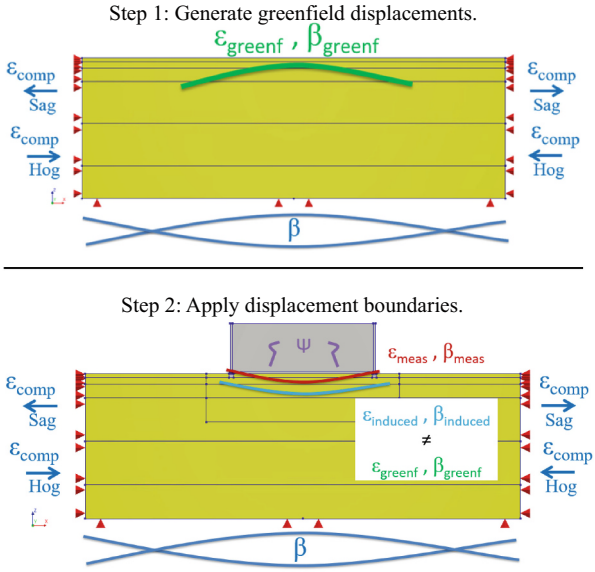


Fig. 4. Two-step approach employed in this study to relate greenfield deformations to building damage.

damage parameter than summarises into a scalar the various cracks considering their width and length [34].

The models employ quadratic solid elements (CHX60) with the Total Strain Rotating Crack Model (TSRCM, [35, 36]) for the homogenised, smeared, constitutive material of the masonry. A density of 1900 kg/m^3 is used, and a Young's modulus of 5 GPa and Poisson's ratio of 0.25 are employed for the elastic behaviour. In tension, a strength of 0.1 MPa with 8.1 N/m as fracture energy, using the Govindjee [37] crack-band-width criterion, is selected. Similarly, in compression, the strength is 8.5 MPa and the fracture energy 18.4 kN/m. The material properties are representative of old, fired-clay brick façades found in the Netherlands [38]. Figure 6 shows the stress-strain relationships for the material model.

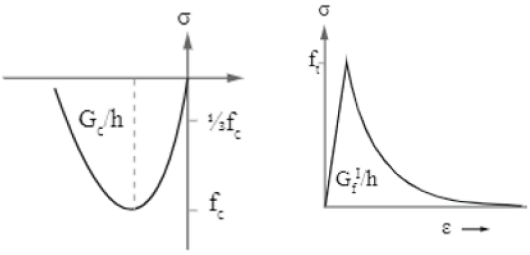


Fig. 6. Stress-strain relationships for compressive and tensile behaviour, respectively [35].

The models are analysed with multiple stages. First, the gravity load and soil consolidation are resolved with a K0 procedure. The construction sequence of the façade is accounted for. Then, the soil deformations are applied to the boundaries of the soil block. At every load step, the relationship between greenfield soil deformations (from the first-tier model) and façade damage (in Ψ from the second-tier model) are registered.

In addition, geometry variations are considered for the façade as per Fig. 7. The intention is to remove the sensitivity of the results to specify geometric properties such as the location and dimension of openings, height and length of the façade, and shape of the roof. In particular, long façades, with large opening percentages are expected to be most vulnerable to damage. These historical façades sport flexible timber floors and roof.

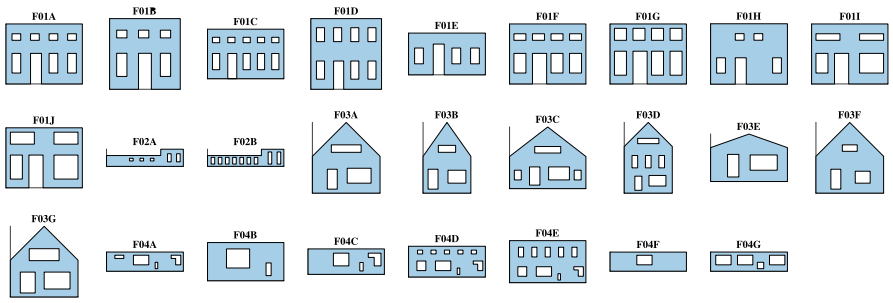


Fig. 7. Geometric variations for the models. Façades with different opening percentages, opening dimensions, varying length/height ratios, and top geometrical shape.

3 Results

The results are exemplified for the standard variation of the façade, F01A with standard material. In Fig. 8, the progressive cracking of the façade is visualised for invisible damage ($\Psi < 1$) where incipient cracks appear at the corners of the windows and at the connections with the transversal walls. Because of the extensive horizontal strain, the transversal walls move apart from each other. Because of the hogging shape, the top of the façade is extended, consequently, the cracks around the windows propagate upwards forming vertical cracks that join neighbouring openings at $\Psi = 2$ (clearly visible damage with several cracks of about 0.5 mm in width). Towards the end of light damage ($\Psi > 3$) cracking has almost split the façade in two.

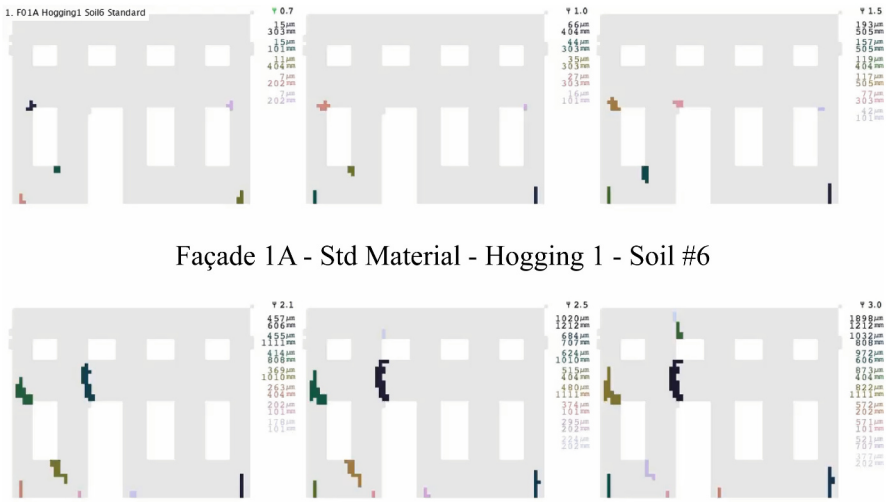


Fig. 8. Crack patterns and automatic Ψ characterisation for an exemplary case of the standard façade on the stiff soil. Hogging shape in combination with extensive horizontal strain.

The greenfield displacement associated with specific values of Ψ can be plotted in a graph similar to that of Boscardin and Cording [31] with the angular distortion on the horizontal axis and the horizontal strain on the vertical axis. For the various material, soil and curvature/strain combinations for the standard façade (F01A), all data points are gathered in Fig. 9. The lines from [31] are included for comparison. The figure shows that for small values of curvature/strain, the associated damage on the façade is also small ($\Psi = 1$). As curvature, strain, or curvature/strain increase, so does damage increase. For a negative horizontal strain, damage is significantly lower; this is expected since the masonry can withstand compressive stresses easily. In these cases, damage arises from the induced bending on the façades. Focusing on the positive strain quadrant, the graph also shows remarkable agreement with the existing limits proposed by Boscardin and Cording [31]. Data points for $\Psi = 1$ are close to the line originating from the study that better matches the description for this damage level. As the second threshold is exceeded, model results also show a $\Psi \geq 2$; ditto for $\Psi \geq 3.5$. For the contraction strain, the lines are too conservative, but these were presumably formulated for the more damaging extensive strain and hogging curvatures.

Since the results of this study not only include façade 1A, but all fired-clay façade variations on masonry foundations shown in Fig. 7, more than 20 000 data points at the indicated Ψ values are available. These can be used to draw exceedance lines for curvature/strain combinations. The exceedance lines are formulated by simply counting the number of models that exceed a given threshold of damage for specific values of greenfield curvature and strain. This is done in Fig. 10. For a given threshold of Ψ ($\Psi = 1$, 1.5, 2, and 3.5), the lines corresponding the 10%, 25% and 50% of the models are presented. The line, for which 50% of the models exceed the given Ψ value, corresponds

to the expected Ψ. The portion of the lines that are too far from model results are considered extrapolations.

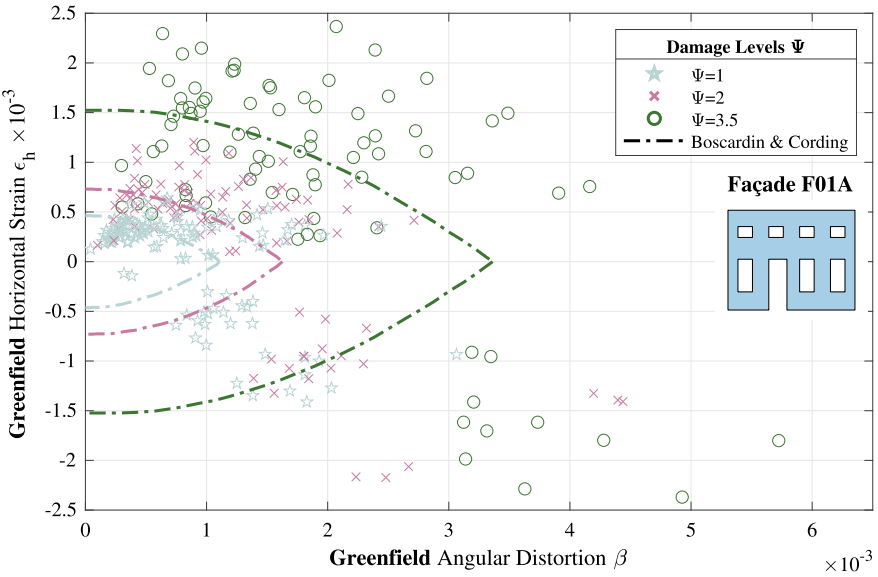


Fig. 9. Data points for three damage levels for façade F01A for curvature/strain combos.

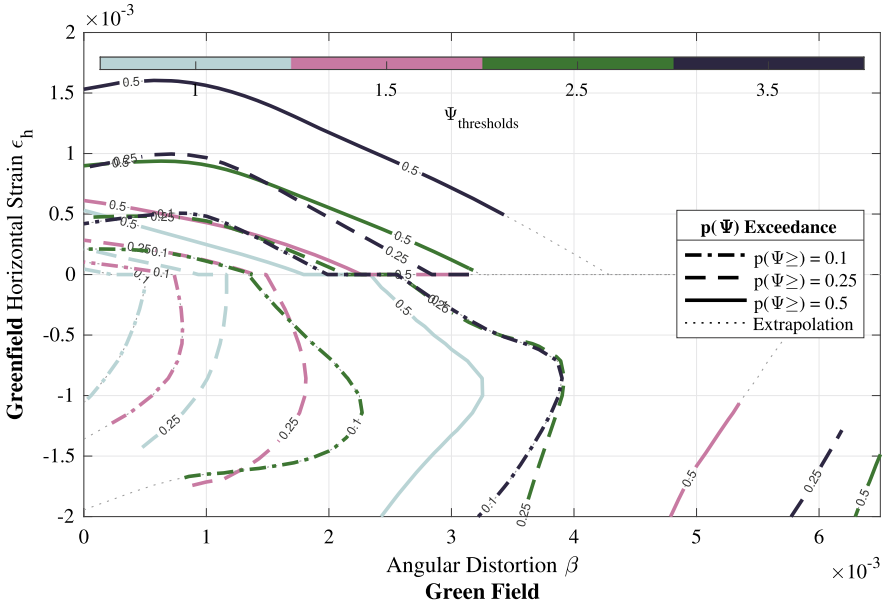


Fig. 10. Exceedance contours for curvature/strain combinations.

First, the figure shows that damage for extensive greenfield strains occurs much earlier than for compressive strains, as observed in Fig. 9. Second, combinations of curvature and strain are more damaging than each individually; this is also expected. At a pure strain of 5e−4, a $\Psi = 1$ is expected and the probability of exceeding light damage ($\Psi \geq 3.5$) is about 10%; if combined with an angular distortion of 2e−3 ($\beta = 1/500$), the expected damage doubles and so does the probability of exceeding light damage. The same curvature/strain in contraction (sagging, negative side) results in a probability of less than 40% of displaying visible cracks ($\Psi = 1$).

The results can be segregated by the distinct parameters varied; in Fig. 11, the influence of the various soil profiles is inspected. In addition, the lines are drawn on a logarithmic scale to better observe their behaviour for small curvatures and strains thus complementing the information provided in Fig. 10. The stiffer, sandy profile (Soil #6) leads to damage earlier for both curvature and strains: already at $\varepsilon_h = 2e{-}4$, visible damage ($\Psi = 1$) is expected, while the softer soils, especially Soil #9, allows deformations up to 5e−4. In general, combinations with an angular distortion up to 3e−4 ($\beta \approx 1/3000$) seem not to increase damage significantly; above this value the compounding effect of combing curvature and strain plays a role.

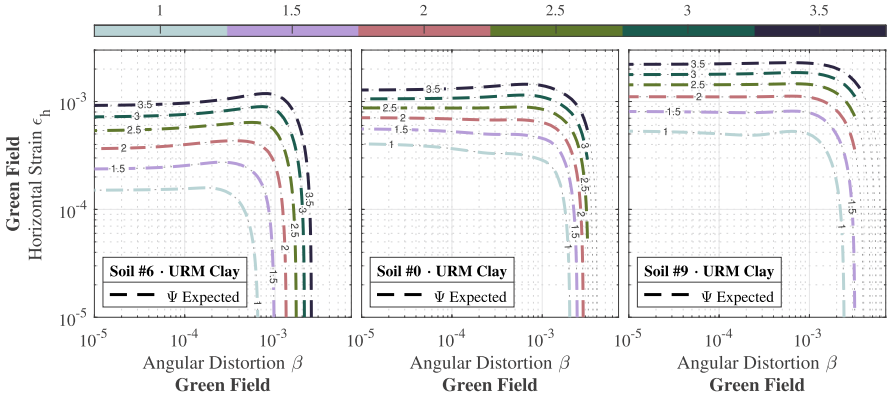


Fig. 11. Exceedance curves segregated by soil profile, on logarithmic axes.

4 Discussion

While this study represents a significant advancement in understanding mining-induced damage, certain limitations remain. The analysis focused primarily on masonry façades, and further research is needed to extend the findings to complete buildings. Multi-wall systems, connections, and roof-structure interactions may introduce additional complexities that require investigation. The study highlights that the non-linear behaviour of masonry structures, that become more flexible as they gather damage, will change the response of the structure-soil system; cracking is therefore important. However, cyclic effects have not been explored; these effects can benefit from a more robust material model such as the EMM [39].

On the other hand, quasi-static deformations on buildings occurring over a long-time span could be adopted by the structure without causing cracks. This time-dependent

phenomenon, called creep, has not been considered in the models and requires further study.

Additionally, only three soil profiles—stiff sand and soft clay/peat—were considered. Although these profiles provide valuable insights, particular soil conditions may exhibit different behaviours. Future studies should explore a broader range of soil types to refine predictions of strain transfer and damage severity. Moreover, the adopted profiles present horizontally-homogeneous layers. Slanted or vertical soil layers, or heterogeneous properties will change the behaviour of the soil-structure system, where localisation of strains may occur. A healthy building could divert localisations while pre-damaged buildings could emphasise their development on a location detrimental to the structure.

The study also relied on proportional loading paths in the curvature-strain space, where strain and curvature were scaled simultaneously. In reality, non-proportional loading scenarios—where strain and curvature evolve at different rates—may occur, particularly in complex subsurface conditions. Similarly, deformations are applied on a plane parallel to the main façade, 3D deformations could lead to differing damage intensity.

The study has considered shallow strip foundations, characteristic of historical façades in the Netherlands. However, piled foundations, supporting the masonry strip on timber planks atop timber piles, are likely to behave differently. While these are less susceptible to heterogenous effects of the soil directly underneath the foundation, they are connected to the stiffer soil layers underneath. For sources relating to deep subsidence, this may increase the deformations transferred to the building. This remains an interesting complementary study. Conversely, reinforced concrete strip or slab foundations are likely to be better prepared to sustain horizontal strain since the embedded rebar provides the structure with adequate strength against horizontal extension strains. Similarly, sagging curvature, which leads to tensile stresses at the bottom of the buildings, where the rebar in the foundation can sustain those stresses, will influence buildings with reinforced foundations less. For hogging and compressive strains, the benefits of reinforced foundations are expected to be less significant, though these cases remain to be explored.

The methodology of the study, comprising the two model tiers, is adequate for soil deformations originating from outside of the modelled soil block. This is because the boundary displacements are applied at the perimeter of the block and the soil-structure interaction develops between the soil modelled and the façade on top. For settlement sources within the soil block, such as consolidation due to increased weight of the structure or soil distortions because of changes in the ground water table occurring directly underneath the structure, this approach may not be valid. The influence in the damage predicted in contrast to sources from outside the soil block is yet to be studied.

The results provide a useful tool to evaluate the combined effects of curvature and horizontal strain on (historical) masonry buildings. This will enable more reliable predictions nearby mining operations, allowing for clearer decision making. Similarly, tunnelling or geothermal projects, which can lead to ground deformations, will benefit from more robust estimates of light damage probability.

Additionally, the results presented can also be used for diagnosis and forensics of existing damage. For example, damage on buildings on soft soils is less likely to originate from deep sources and relate instead to shallow soil settlements.

Indeed, despite the aforementioned limitations, the study provides a strong foundation for future research. Key recommendations include extending the models to full buildings, incorporating additional soil profiles, and validating predictions through in-situ measurements and manipulative testing. Such efforts will further improve our understanding of ground-structure interactions and support the development of practical guidelines for damage assessment and mitigation.

5 Conclusions

This study has provided significant insights into the response of historical masonry façades to ground-induced deformations, particularly highlighting their vulnerability when subjected to combined curvature and horizontal strain. The research underscored the importance of accurately modelling the non-linear and progressive damage behaviour of masonry, as increased damage results in higher structural flexibility, influencing the interaction between the building and underlying soil.

It was established that the combination of curvature and horizontal strain leads to more severe damage than each effect individually, emphasising the necessity for considering multiple deformation sources concurrently when evaluating building vulnerability. The findings also showed considerable variation in damage severity depending on the soil stiffness, with stiffer soils transferring deformation to façades more aggressively, thus causing earlier and more significant cracking.

Despite its valuable contributions, the study recognises several limitations, including assumptions about quasi-static loading conditions, omission of creep effects, and simplifications in foundation types and soil profiles. Therefore, future research should explore these aspects, including cyclic loading scenarios, diverse soil conditions, and more complex foundation configurations. Additionally, validating numerical results with empirical data and field observations will further enhance the practical applicability of the findings.

Ultimately, this research represents a meaningful step toward a more comprehensive understanding of ground-structure interaction effects on historical masonry buildings. It provides practical guidance for risk assessment and management in areas affected by mining, tunnelling, or geothermal activities and serves as a foundational basis for further studies aimed at safeguarding the integrity and heritage value of historical structures.

Acknowledgements. Participation and funding provided by Instituut Mijnbouwschade Groningen (IMG) and Commissie Mijnbouwschade (CM) is gratefully acknowledged.

References

1. Prosperi, A., Longo, M., Korswagen, P.A., Korff, M., Rots, J.G.: 2D and 3D modelling strategies to reproduce the response of historical masonry buildings subjected to settlements. Int. J. Archit. Herit. (2024). https://doi.org/10.1080/15583058.2024.2325472

2. Puncello, I., Caprili, S.: Seismic assessment of historical masonry buildings at different scale levels: a review. Appl. Sci. **2023**(13), 1941 (2023). https://doi.org/10.3390/app13031941
3. Korswagen, P.A., Longo, M., Prosperi, A., Rots, J.G., Terwel, K.C.: Modelling of damage in historical masonry façades subjected to a combination of ground settlement and vibrations. In: SAHC 2023, RILEM Bookseries, vol. 47, pp. 904–917 (2023). https://doi.org/10.1007/978-3-031-39603-8_73
4. Valente, M., Milani, G.: Damage assessment and collapse investigation of three historical masonry palaces under seismic actions. Eng. Fail. Anal. **98**, 10–37 (2019). https://doi.org/10.1016/j.engfailanal.2019.01.066
5. Sandoval, C., Valledor, R., Lopez-Garcia, D.: Numerical assessment of accumulated seismic damage in a historic masonry building. A case study. Int. J. Archit. Herit. **11**(8), 1177–1194 (2017). https://doi.org/10.1080/15583058.2017.1356945
6. Korswagen, P.A., Longo, M., Rots, J.G., Terwel, K.C.: Sensitivity of damage accumulation of masonry walls due to earthquake vibrations via finite-element models. In: 14th North American Masonry Conference (NAMC), Nebraska, USA (2023)
7. Mosoarca, M., Keller, A.I., Petrus, C., Racolta, A.: Failure analysis of historical buildings due to climate change. Eng. Failure Anal. **82**, 666–680 (2017). https://doi.org/10.1016/j.engfailanal.2017.06.013
8. Groot, C.J.W.P., Gunneweg, J.T.M.: Choosing mortar compositions for repointing of historic masonry under severe environmental conditions. In: Hughes, J., Válek, J., Groot, C. (eds.) Historic Mortars. Springer, Cham (2019). https://doi.org/10.1007/978-3-319-91606-4_11
9. van Thienen-Visser, K., Breunese, J.N.: Induced seismicity of the Groningen gas field: History and recent developments. In: The Leading Edge June 2015 Special Section: Injection-induced seismicity (2015). https://doi.org/10.1190/tle34060664.1
10. Korswagen, P.A., Longo, M., Meulman, E., Rots, J.G.: Crack initiation and propagation in unreinforced masonry specimens subjected to repeated in-plane loading during light damage. Bull. Earthq. Eng. (2019). https://doi.org/10.1007/s10518-018-00553-5
11. Korswagen, P., Longo, M., Meulman, E., Rots, J.G.: Experimental and computational study of the influence of pre-damage patterns in unreinforced masonry crack propagation due to induced, repeated earthquakes. In: 13th North American Masonry Conference (2019)
12. Van Staalduinen, P.C., Terwel, K., Rots, J.G.: Onderzoek naar de oorzaken van bouwkundige schade in Groningen Methodologie en case studies ter duiding van de oorzaken. Delft University of Technology. Report number CM-2018-01 (2018). www.NationaalCoordinatorGroningen.nl
13. Burland, J.B., Broms, B.B., Mello, V.F.B.D.: Behaviour of foundations and structures. Build. Res. Establish. (1977)
14. Burland, J.B., Standing, J.R., Jardine, F.M.: Building Response to Tunnelling Case Studies from Construction of the Jubilee Line Extension, p. 200. CIRIA Special Publication, London (2001)
15. Li, J., Guo, L.: Field investigation and numerical analysis of residential building damaged by expansive soil movement caused by tree root drying. J. Perform. Constr. Facil. **31**(1), D4016003 (2017). https://doi.org/10.1061/(ASCE)CF.1943-5509.0000908
16. Peduto, D., Nicodemo, G., Maccabiani, J., Ferlisi, S.: Multi-scale analysis of settlement-induced building damage using damage surveys and DInSAR data: a case study in The Netherlands. Eng. Geol. **218**, 117–133 (2017). https://doi.org/10.1016/j.enggeo.2016.12.018
17. Tong, J., Sun, X., Jia, N., Dang, W., Li, Z.: Analysis of settlement of existing buildings caused by unreasonable design of foundation. In: IOP Conference Series: Earth and Environmental Science, vol. 371, p. 022031 (2019). https://doi.org/10.1088/1755-1315/371/2/022031
18. Wei, H.: Influence of foundation pit excavation and precipitation on settlement of surrounding buildings. Adv. Civ. Eng. **2021**, Article ID 6638868 (2021). https://doi.org/10.1155/2021/6638868

19. Yong, C.Z., Denys, P.H., Pearson, C.F.: Groundwater extraction-induced land subsidence: a geodetic strain rate study in Kelantan, Malaysia. J. Spat. Sci. **64**(2), 275–286 (2019). https://doi.org/10.1080/14498596.2018.1429329
20. Burland, J.B., Wroth, C.P.: Settlement of buildings and associated damage. In: Proceedings of Conference on Settlement of Structures, pp. 611–654. Pentech Press, Cambridge (1974)
21. Mair, R.J.: Research on tunnelling-induced ground movements and their effects on buildings – lessons from the Jubilee Line extension. In: Burland J.B., Standing J.R., Jardine F.M. (eds.) Building Response to Tunnelling: Case Studies from Construction of the Jubilee Line Extension. CIRIA SP199 and Thomas Telford, London (2003)
22. Budhu, M., Adiyaman, I.B.: Mechanics of land subsidence due to groundwater pumping. Int. J. Numer. Anal. Meth. Geomech. **34**, 1459–1478 (2010). https://doi.org/10.1002/nag.863
23. Son, M., Cording, E.J.: Estimation of building damage due to excavation-induced ground movements. J. Geotech. Geoenviron. Eng. (2005)
24. Skempton, A.W., MacDonald, D.H.: The allowable settlements of buildings. Proc. Inst. Civ. Eng. **5**, 727–768 (1956)
25. Tandanand, S., Powell, L.R.: Determining horizontal displacement and strains due to subsidence. United States Department of the Interior - Ri 9358 (1991)
26. Heib, M.A., Linkov, A.M., Zoubkov, V.V.: On numerical modeling of subsidence induced by mining. In: International Symposium of the International Society for Rock Mechanics (EUROCK 2001), Espoo, Finland. ineris-00972217 (2014)
27. Barbato, J., Hebblewhite, B., Mitra, R., Mills, K.: Prediction of horizontal movement and strain at the surface due to longwall coal mining. Int. J. Rock Mech. Min. Sci. **84**, 105–118 (2016). https://doi.org/10.1016/j.ijrmms.2016.02.006
28. Deck, O., Anirudh, H.: Numerical study of the soil–structure interaction within mining subsidence areas. Comput. Geotech. **37**, 802–816 (2010). https://doi.org/10.1016/j.compgeo.2010.07.001
29. Ritter, S., Giardina, G., Franza, A., DeJong, M.J.: Building deformation caused by tunneling: centrifuge modeling. J. Geotech. Geoenviron. Eng. (2020). https://doi.org/10.1061/(ASCE)GT.1943-5606.0002223
30. Franzius, J.N., Potts, D.M., Burland, J.B.: The response of surface structures to tunnel construction. P I Civ. Eng.-Geotech. **159**(1), 3–17 (2006). https://doi.org/10.1680/geng.2006.159.1.3
31. Boscardin, M.D., Cording, E.J.: Building response to excavation-induced settlement. J. Geotech. Eng. **115**(1), 1–21 (1989)
32. Tzenkov, A.D., Schwager, M.V.: Nonlinear FEM analysis of the seismic behavior of the menta bituminous-face rockfill dam. In: Numerical Analysis of Dams. Lecture Notes in Civil Engineering, vol. 91 (2021). https://doi.org/10.1007/978-3-030-51085-5_35
33. Prosperi, A., Korswagen, P.A., Korff, M., Schipper, R., Rots, J.G.: Empirical fragility and ROC curves for masonry buildings subjected to settlements. J. Build. Eng. **68**, 106094 (2023). https://doi.org/10.1016/j.jobe.2023.106094
34. Korswagen, P.A., Rots, J.G.: Monitoring and quantifying crack-based light damage in masonry walls with digital image correlation. In: Proceedings of 1st International Conference on Structural Damage Modelling and Assessment. Lecture Notes in Civil Engineering, vol. 110 (2020). https://doi.org/10.1007/978-981-15-9121-1_1
35. Rots, J.G.: Smeared and discrete representations of localized fracture. Int. J. Fract. **51**, 45–59 (1990). https://doi.org/10.1007/BF00020852
36. Rots, J.G., Messali, F., Esposito, R., Jafari, S., Mariani, V.: Computational modelling of masonry with a view to Groningen induced seismicity. In: 10th SAHC Structural Analysis of Historical Construction, Leuven (2016)
37. Govindjee, S., Kay, G.J., Simo, J.C.: Anisotropic modelling and numerical simulation of brittle damage in concrete. Int. J. Numer. Methods Eng. **38**, 3611–3633 (1995)

38. Jafari, S., Esposito, R., Rots, J.G., Messali, F.: Characterizing the material properties of Dutch unreinforced masonry. Procedia Eng. **193**, 250–257 (2017)
39. Sousamli, M.: Orthotropic cyclic continuum constitutive model for masonry structures and comparative studies. TU Delft (2024)
40. Lee, K.L., Shen, C.K.: Horizontal movements related to subsidence. J. Soil Mech. Found. Div. (1969)